Work-hardening behavior of commercially pure titanium JIS grade 1 sheet upon reverse loading

Takayuki Hama' , Ning Yi' , Akihiro Kobuki' , Sohei Uchida' , Hitoshi Fujimoto' , and Hirohiko Takuda'

Citation: AIP Conference Proceedings **1769**, 200001 (2016); doi: 10.1063/1.4963619
View online: http://dx.doi.org/10.1063/1.4963619
View Table of Contents: http://aip.scitation.org/toc/apc/1769/1
Published by the American Institute of Physics

Work-Hardening Behavior of Commercially Pure Titanium JIS Grade 1 Sheet upon Reverse Loading

Takayuki Hama[1, a)], Ning Yi[1, 2, b)], Akihiro Kobuki[1, c)], Sohei Uchida[3, d)] Hitoshi Fujimoto[1, e)], and Hirohiko Takuda[1, f)]

[1]*Graduate school of Energy Science, Kyoto University, Yoshida-honmachi, Sakyo-ku, Kyoto 606-8501, Japan*
[2]*School of Materials Science and Engineering, Beijing Institute of Technology, Beijing 100081, China*
[3]*Technology Research Institute of Osaka Prefecture, 7-1, Ayumino-2, Izumi, Osaka 597-1157, Japan*
[a)]Corresponding author: hama@energy.kyoto-u.ac.jp
[b)] yi.ning@outlook.com
[c)] kobuki.akihiro.48v@st.kyoto-u.ac.jp
[d)] UchidaS@tri-osaka.jp
[e)] h-fujimoto@energy.kyoto-u.ac.jp
[f)] takuda@energy.kyoto-u.ac.jp

Abstract. In the present study, work-hardening behavior under various loading paths of a commercially pure titanium JIS Grade 1 sheet was investigated. The following tension-compression asymmetry was presented. The yield stress was smaller under compression than under tension, whereas the subsequent work-hardening was larger under compression than under tension. When the sheet was subjected to reverse loading from compression to tension, strong Bauschinger effect was exhibited. Thereafter, a concave curve followed by a small stress peak appeared, which was not presented under monotonic tension. Microstructure observations suggested that this characteristic behavior would be owing to the the activities of twinning and detwinning respectively during compression and following tension.

INTRODUCTION

Commercially-pure titanium (CP-Ti) sheets have various features such as good drawability, high specific strength, and high corrosion resistance; thus, CP-Ti sheets are receiving increasing attention in various industries including for aircraft and automobile applications [1, 2].

CP-Ti sheets are a hexagonal-close-packed (hcp) metal, and the critical resolved shear stress and work-hardening differ notably depending on the slip and twinning systems. Moreover, to fulfill the von Mises criterion, the activity of twinning systems plays an important role in the deformation behavior [3, 4]. Because of the strong crystal anisotropy of hcp structure and the polar character of twinning, CP-Ti sheets present strongly anisotropic-deformation behavior. Furthermore, a strong basal texture is generally developed in rolled CP-Ti sheets; thus, the anisotropy is further pronounced. A lot of studies were conducted to understand the anisotropic-deformation behavior of CP-Ti sheets [5-12].

Sheet metals generally experience strain-path changes including reverse loading during sheet forming. Therefore, it is important to understand the deformation behavior under not only monotonic loading paths but also strain-path changes. Thus far, most of the studies focused on the deformation behavior under monotonic tension or compression [6-12]. In our previous study [5], the work-hardening and twinning behaviors under various loading paths including reverse loading in a CP-Ti JIS Grade 2 sheet were investigated. It was found that the Bauschinger effect was presented under both tension followed by compression and compression followed by tension (compression-tension). Moreover, during tension following compression $<10\bar{1}2>$ detwinning was active as for Mg alloy sheets that also had the hcp structure. In contrast, the effect of detwinning activity on the work-hardening behavior was much

ESAFORM 2016
AIP Conf. Proc. 1769, 200001-1–200001-5; doi: 10.1063/1.4963619
Published by AIP Publishing. 978-0-7354-1427-3/$30.00

smaller in the CP-Ti Grade 2 sheet than in Mg alloy sheets. This difference would presumably because the twinning and detwinning activities were much less pronounced in the CP-Ti Grade 2 sheet than in Mg alloy sheets.

In the meanwhile, CP-Ti sheets are classified into several grades depending on the additive amounts of oxygen and iron: the grade number becomes large as the additive amounts increase. It is known that twinning activity increases as the additive amounts decrease, i.e., twinning activity is more pronounced in Grade 1 sheets than in Grade 2 sheets. Therefore, it is expected that the effect of twinning and detwinning activities on the work-hardening behavior would also be more pronounced in Grade 1 sheets than in Grade 2 sheets. However, the deformation behavior of Grade 1 sheets under reverse loading has not been studied; thus, its detail is not yet understood.

In the present study, the work-hardening behavior of a CP-Ti Grade 1 sheet is investigated particularly focusing on reverse loading. Electron backscatter diffraction (EBSD) is used to study twinning and detwinning activities during deformation. Moreover, the difference in the work-hardening behavior between Grade 1 and Grade 2 sheets is also discussed.

EXPERIMENTAL PROCEDURE

A cold rolled CP-Ti JIS Grade 1 sheet (Kobe steel) was used. The nominal thickness was 1.0 mm. Tests of monotonic tension, monotonic compression, and reverse loading were conducted in the rolling direction (RD). In the reverse loading test, the sheet was first subjected to compression followed by tension (compression-tension). This loading path was selected because it was presented in our past study for a Grade 2 sheet [5] that activities of $<10\bar{1}2>$ twinning and detwinning were observed during compression-tension. To prevent buckling during compression, comb-shaped dies [13,14] were employed to give compressive forces through the thickness of the sheet. The schematic diagrams of the experimental apparatus and the sample geometry are presented in Fig. 1. The through-thickness stress applied to the sheet was approximately 3.6 MPa, which corresponded to approximately 3 % of the initial yield stress of the sheet. Molybdenum disulfide (Moly paste, Sumico Lubricant Co.) was utilized for lubrication between the sheet and the comb-shaped dies. A strain gauge (KFEM, Kyowa Electronic Instruments) was employed for the strain measurement during the test. The test was conducted at the initial strain rate of approximately $6.67 \times 10^{-4}/\mathrm{s}^{-1}$ at room temperature.

After the reverse loading test was carried out, the microstructures of the samples were measured using EBSD on cross-sectional surfaces perpendicular to the RD. The pole figure (PF) and inverse pole figure map (IPF map) were analyzed using OIM-Analysis 7 (TSL Solutions).

RESULTS AND DISCUSSION

Stress-strain curves

Fig. 2 (a) shows the true stress-strain curves obtained under monotonic tension and compression. Note that absolute stress and absolute strain are used in this figure. The yield stress is smaller under compression than under

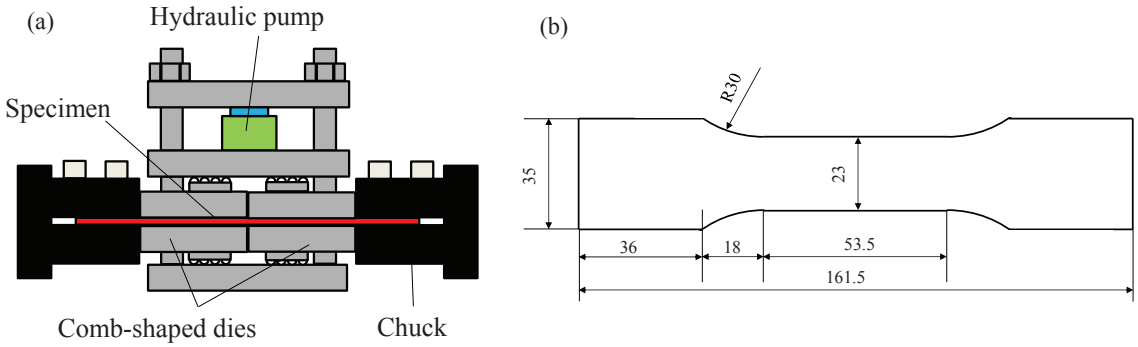

Fig. 1 Schematic diagrams of (a) experimental apparatus and (b) sample geometry (in mm).

tension, whereas the subsequent work-hardening is larger under compression than under tension. Apparently, a strong tension-compression asymmetry is presented. This result is consistent with that reported in the literature [12]. Fig. 2 (b) displays the result of compression-tension. The amount of nominal strain imparted before the strain reversal was either 5% or 10 %. The Bauschinger effect is exhibited after the strain reversal. Thereafter, a concave curve followed by a small stress peak appears. This curve occurs irrespective of the amount of the pre-strain. Interestingly, this curve does not occur under monotonic tension (Fig. 2 (a)), describing that a strain-path dependency is presented.

When a Grade 2 sheet was subjected to compression-tension, strong Bauschinger effect was also presented, whereas neither the concave curve nor the stress peak was exhibited [5].

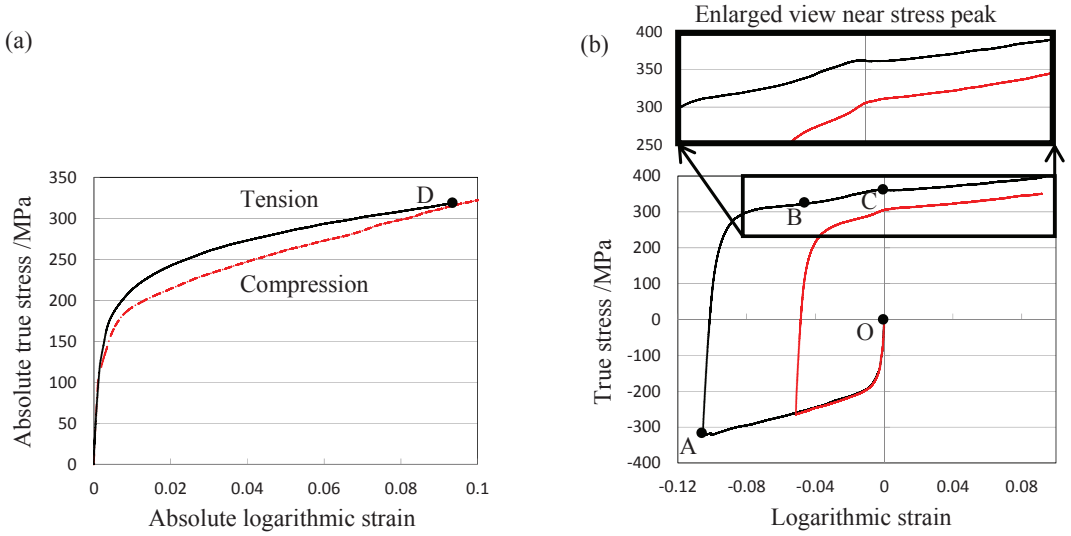

Fig. 2 Stres-strain curves. (a) Monotonic tension and monotonic compression, and (b) compression-tension.

Microstructures

Next, the results of EBSD measurement are described [15]. The measurement was conducted at points O, A, B, C, and D designated in Fig. 2. Fig. 3 (a) shows the initial PF and IPF map (point O). The typical basal texture appears, and twinning is hardly presented. Figs. 3 (b) and 3 (c) display respectively the results obtained under monotonic compression (point A) and monotonic tension (point D). Note that boundaries of $<10\bar{1}2>$, $<11\bar{2}1>$, and $<11\bar{2}2>$ twinning systems are designated respectively with red, green, and blue lines in the IPF map. $<10\bar{1}2>$ twinning is very active when the sheet is subjected to compression, resulting in the strong peaks in the RD in the PF. In contrast, $<11\bar{2}2>$ twinning is active when the sheet is subjected to tension, but the PF remains almost unchanged from that of the initial one. Apparently, the active twin mode is different between tension and compression. Moreover, the activity of $<10\bar{1}2>$ twinning under compression is more pronounced than that of $<11\bar{2}2>$ twinning under tension.

Figs. 3 (d) and 3 (e) depict the results obtained after the loading direction is inverted from compression to tension (points B and C). The area fraction of $<10\bar{1}2>$ twinning decreases notably from point A to point B, i.e., detwinning is active from point A to point B; thus, the strong peaks in the RD observed at point A disappear mostly at point B. At point C, $<10\bar{1}2>$ detwinning is almost completed, while $<11\bar{2}2>$ twinning starts activating.

Comparing the results between the Grade 1 and Grade 2 sheets [5], the abovementioned trends in the twinning activity are qualitatively the same. In contrast, the activities of $<10\bar{1}2>$ twinning and $<11\bar{2}2>$ twinning are much more pronounced in the Grade 1 sheet than in the Grade 2 sheet.

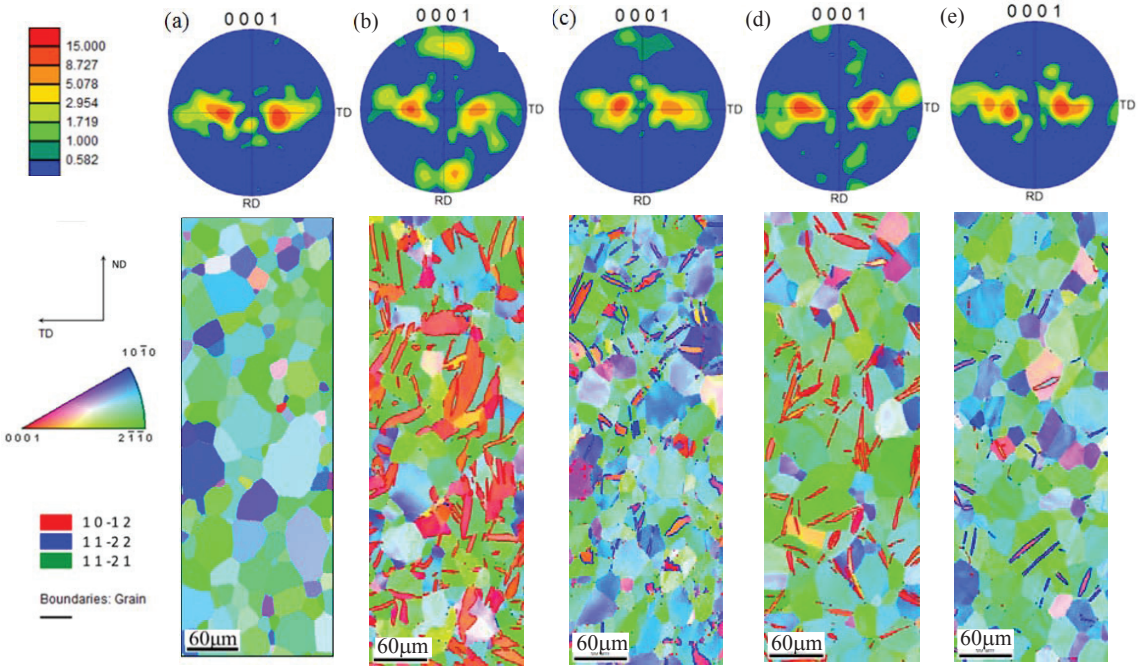

Fig. 3 Results of EBSD measurement at (a) point O, (b) point A, (c) point D, (d) point B, and (e) point C.

Discussion

The mechanism that the characteristic work-hardening behavior occurs under compression-tension is discussed in terms of the microstructure evolution. It is established that a sigmoidal stress-strain curve is presented when Mg alloy sheets that have the hcp structure are subjected to compression-tension [13, 16, 17]. This work-hardening behavior in Mg alloy sheets results from the fact that <10$\bar{1}$2> detwinning is active until the second rapid increase in stress occurs, whereas it is hardly active beyond the second rapid increase [18-20]. The present microstructure observation suggests that the concave curve and the small stress peak that appear in the CP-Ti Grade 1 sheet can also be explained from a similar mechanism: <10$\bar{1}$2> detwinning is active until the stress peak occurs (Fig. 3 (d)), whereas it is hardly active beyond the stress peak (Fig. 3 (e)). Note that the difference in the stress between before and after the stress peak occurs is much smaller in the CP-Ti Grade 1 sheet than that between before and after the second rapid increase in Mg alloy sheets. This small difference in the stress may be because the difference in critical resolved shear stresses among the slip and twinning systems is much smaller in the CP-Ti Grade 1 sheet than in Mg alloy sheets.

As explained before, the Grade 2 sheet did not present either the concave curve or the stress peak. This result may be because twinning and detwinning activities were much less pronounced in the Grade 2 sheet than in the Grade 1 sheet. From these results and discussion, it is concluded that detwinning activity affects the stress-strain curves also in CP-Ti sheets if its activity is large, whereas its effect is essentially smaller in CP-Ti sheets than in Mg alloy sheets.

CONCLUSIONS

The work-hardening and twinning behaviors of a CP-Ti Grade 1 sheet was investigated experimentally. The difference in the deformation behaviors between the Grade 1 and Grade 2 sheets was also discussed. The results obtained in this study are summarized as follows.

(1) When the sheet is subjected to compression followed by tension in the RD, a concave shape followed by a small stress peak is presented in the stress-strain curve. This behavior does not occur in the Grade 2 sheet.

(2) <$10\bar{1}2$> twinning and <$11\bar{2}2$> twinning are active respectively during compression and tension. When the sheet is subjected to strain reversal from compression to tension, <$10\bar{1}2$> detwinning is active in the initial stage of tension, whereas it is hardly active in the latter stage. These trends in twinning activities are the same as those in the Grade 2 sheet, while they are much more pronounced in the Grade 1 sheet than in the Grade 2 sheet.
(3) The concave curve and the small stress peak that appear under tension following compression would result presumably from the following mechanism: <$10\bar{1}2$> detwinning is active until the stress peak occurs, whereas it is hardly active beyond the stress peak. This work-hardening behavior does not present in the Grade 2 sheet because twinning and detwinning activities are much less in the Grade 2 sheet. It is concluded that detwinning activity affects the stress-strain curves in CP-Ti sheets if its activity is large.

ACKNOWLEDGMENTS

This work was partially supported by JSPS KAKENHI Grant Number 26289271 and the Photon and Quantum Basic Research Coordinated Development Program from the Ministry of Education, Culture, Sports, Science and Technology, Japan.

REFERENCES

1. H. Fujii, K. Takahashi and Y. Yamashita, Nippon Steel Tech. Rep., 62-67 (2003).
2. F.H. Froes, H. Friedrich, J. Kiese and D. Bergoint, JOM **56**, 40-44 (2004).
3. X. G. Deng, S. X. Hui, W. J. Ye and X. Y. Song, Mater. Sci. Eng. A **575**, 15-20 (2013).
4. M. Tritschler, A. Butz, D. Helm, G. Falkinger and J. Kiese, Inter. J. Mater. Form. **7**, 259-273 (2014).
5. T. Hama, H. Nagao, A. Kobuki, H. Fujimoto and H. Takuda, Mater. Sci. Eng. A **620**, 390-398 (2015).
6. A. A. Salem, S. R. Kalidindi and R. D. Doherty, Acta Mater. **51**, 4225-4237 (2003).
7. S. Nemat-Nasser, W. G. Guo and J. Y. Cheng, Acta Mater. **47**, 3705-3720 (1999).
8. D. R. Chichili, K. T. Ramesh and K. J. Hemker, Acta Mater. **46**, 1025-1043 (1998).
9. H. Becker and W. Pantleon, Comp. Mater. Sci. **76**, 52–59 (2013).
10. N. Benmhenni, S. Bouvier, R. Brenner, T. Chauveau and B. Bacroix, Mater. Sci. Eng. A **573**, 222-233 (2013).
11. M. Ishiki, T. Kuwabara and Y. Hayashida, J. Mater. Process. Tech. **80**, 517-523 (1998).
12. M.E. Nixon, O. Cazacu and R.A. Lebensohn, Int. J. Plasticity **26**, 516-532 (2010).
13. T. Hama, Y. Kariyazaki, N. Hosokawa, H. Fujimoto and H. Takuda, Mater. Sci. Eng. A **551**, 209-217 (2012).
14. T. Kuwabara, Y. Kumano, J. Ziegelheim and I. Kurosaki, Int. J. Plasticity **25**, 1759–1776 (2009).
15. N. Yi, T. Hama, A. Kobuki, H. Fujimoto, and H. Takuda, Mater. Sci. Eng. A **655**, 70-85 (2016).
16. T. Hama, H. Nagao, Y. Kuchinomachi and H. Takuda, Mater. Sci. Eng. A **591**, 69-77 (2014).
17. X.Y. Lou, M. Li, R.K. Boger, S.R. Agnew and R.H. Wagoner, Int. J. Plasticity **23**, 44-86 (2007).
18. T. Hama, N. Kitamura and H. Takuda, Mater. Sci. Eng. A **583**, 232-241 (2013).
19. T. Hama, T. Mayama and H. Takuda, Romanian J. Tech. Sci. Applied Mech. **60**, 16 pages (2015).
20. T. Hama and H. Takuda, Steel Res. Int. Sp. Ed., 1115-1118 (2012).